



Multicellularity makes the difference: multicellular magnetotactic prokaryotes have dynamic motion parameters dependent on the magnetic field intensity

Ana Luiza Carvalho¹, Fernanda Abreu², Daniel Acosta-Avalos^{1,a} 

¹ Centro Brasileiro de Pesquisas Físicas - CBPF, Rua Xavier Sigaud 150, Urca, Rio de Janeiro, RJ 22290-180, Brazil

² Instituto de Microbiologia Paulo de Góes, Universidade Federal Do Rio de Janeiro - UFRJ, Rio de Janeiro, RJ 21941-902, Brazil

Received: 28 August 2020 / Accepted: 1 February 2021

© The Author(s), under exclusive licence to Società Italiana di Fisica and Springer-Verlag GmbH Germany, part of Springer Nature 2021

Abstract Magnetotactic microorganisms can be found as unicellular entities, as coccus, vibrios, spirilla, rods and protists as well as multicellular organisms. The most studied multicellular magnetotactic prokaryote is “*Candidatus Magnetoglobus multicellularis*,” composed by an average number of 17 genetically identical magnetotactic bacteria. It is known that the magnetotactic orientation of “*Ca. M. multicellularis*” is different from the orientation shown by uncultured magnetotactic cocci. The present manuscript has the aim to compare the dynamic parameters of motion of both the magnetotactic microorganisms. U-turns trajectories were recorded, and one branch of the turn was used to get the trajectory parameters. The individual magnetic moment was estimated using the U-turn diameter. The parameters analyzed were the rotational drag coefficient, the kinetic energy, the flagellar force and the flagellar output power. From the rotational drag coefficient analysis, it was observed a difference among the experimental value and the expected value, and an “effective radius” is proposed to explain that difference. It was observed for the uncultured magnetotactic cocci that the kinetic energy, flagellar force and flagellar power are independent of the magnetic field intensity but for “*Ca. M. multicellularis*” an increase in these values was observed with the magnetic field intensification. It is proposed that the distribution of magnetic moments around the body of “*Ca. M. multicellularis*” is responsible for some magnetic force acting on its body in the presence of a uniform magnetic field. Also, the dynamic motion parameters calculated must support studies on the dynamic of motion of microorganisms.

1 Introduction

Magnetotaxis is the passive alignment of the movement trajectory of a cell along magnetic field lines, which is commonly observed in magnetotactic bacteria (MTB) [1]. That is possible because of the magnetosomes, which are internal organelles that consists in membrane

Electronic supplementary material The online version contains supplementary material available at <https://doi.org/10.1140/epjp/s13360-021-01187-4>.

^a e-mail: dacosta00@gmail.com (corresponding author)

bounded magnetic nanoparticles of the iron oxide magnetite (Fe_3O_4) or the iron sulfide greigite (Fe_3S_4). Magnetosomes are organized in linear chains inside the cytoplasm, and that chain confers to the microorganism a magnetic moment, allowing its interaction with magnetic fields [2]. In the presence of a uniform magnetic field, the only interaction is a torque that aligns the magnetic moment and the cellular body to the magnetic field direction [3]. That happens because the magnetosome chain produces a magnetic moment that is uniform inside the bacterial body, producing a constant magnetic energy in the presence of a uniform magnetic field and whose spatial gradient is null, producing a null magnetic force. The magnetic torque is transmitted from the magnetosome chain to the MTB body through the cytoskeleton filaments [4]. The magnetic field does not push the cellular body, and it only orients the bacterial movement and does not modifies their velocity [3]. Keim et al. [5] showed that the translation velocity of the multicellular magnetotactic prokaryote “*Ca. M. multicellularis*” maintains its average value from 0.9 Oe to 32 Oe, different that was shown by Almeida et al. [6] where a significant increase in the velocity of the same microorganism is observed from 3.9 to 20 Oe and also shown by De Melo and Acosta-Avalos [7] that showed an increase in the velocity from 1.6 to 26.6 Oe. Pichel et al. [8] show that the velocity of *Magnetospirillum gryphiswaldense*, a unicellular magnetotactic bacterium, is statistically similar from 10 to 120 Oe. For an uncultured unicellular MTB collected from a river in Marica city, Rio de Janeiro, Brazil, it has been observed that the translation velocity does not change significantly for magnetic fields from 2.1 to 4.6 Oe [9] and also for an uncultured MTB cocci collected in Lagoa Rodrigo de Freitas, Rio de Janeiro, Brazil, for magnetic fields between 0.59 and 0.72 Oe [10]. In those papers, the dynamical parameters of the movement, in particular the kinetic energy, were not estimated. As the magnetic field does not exert any force on the MTB, the kinetic energy must have a constant average value for a population when the magnetic field changes, meaning also that the hydrodynamical power $P = F_{\text{Hydro}} \cdot v$ (related to the output power of the flagellar motor) must be independent of the magnetic field. Pierce et al. [11] using micromagnetic tweezers measured the swimming velocity, the propulsive force and the output power of the flagellar motor for *Magnetospirillum magneticum* strain AMB-1 and observed that the power of the flagellar motor has a strong positive correlation with the magnetic moment, associating this correlation with a higher metabolism related to the production of more magnetosomes and to higher flagellar power [11]. In the present paper, the kinematics and dynamics of the movement of two different magnetotactic microorganisms is described by observing their swimming trajectories as a function of the magnetic field, measuring their velocities, trajectory orientation, effective temperature, drag coefficient, flagellar power output P_{Fla} , flagellar force F_{Fla} and kinetic energy K . The best way to estimate the kinetic energy through the trajectory analysis is to study spherical organisms because it is necessary to estimate the mass of the microorganism. For a spherical body, its mass M is equal to $(4/3)\pi R^3 \rho$, where R is the body radius and ρ is the body density. Considering that the bacterial body is almost entirely composed by water, then $\rho = 10^3 \text{ kg/m}^3$. The kinetic energy is defined as:

$$K = (1/2)M V_T^2 + (1/2)I \omega^2. \quad (1)$$

The first term corresponds with the energy associated with translation and the second one to the body rotation. V_T is the translational velocity, M is the mass, I is the moment of inertia, and ω is the body angular velocity. For a body rotation axis passing through the center of mass, the moment of inertia can be written as $I_{\text{CM}} = (2/5)MR^2$. The kinetic energy is involved

in the work-energy theorem that states that the work done for all the forces acting on a body is equal to the change of kinetic energy K :

$$W_{\text{Total}} = \Delta K. \quad (2)$$

For a bacterium, the only forces acting are the flagellar and hydrodynamic forces whose sum is zero, meaning that there is no net work done on the bacterial body: $W_{\text{Flagella}} = -W_{\text{Hidro}}$, and K must be constant, not depending on the external magnetic field. The aim of the present paper is to describe the dynamical parameters of the movement of magnetotactic microorganisms and to challenge the idea that K does not depend on the magnetic field, measuring it as stated by Eq. (1) for two different spherical magnetotactic microorganisms: an uncultured MTB coccus and the multicellular magnetotactic prokaryote “*Ca. M. multicellularis*”.

2 Materials and methods

Water and sediment containing “*Ca. M. multicellularis*” were collected in Araruama lagoon, Rio de Janeiro State, Brazil (22° 55′ 24″ S, 42° 18′ 12″ W) and maintained in glass aquariums in the laboratory for several weeks. Uncultured MTB cocci were collected in Rodrigo de Freitas lagoon (22° 58′ S, 43° 12′ W), an urban lagoon located in Rio de Janeiro city. These sediments were collected in 2007 and have been maintained in a glass aquarium since then, completing the aquarium water level from time to time using tap water. The local geomagnetic parameters where “*Ca. M. multicellularis*” and the uncultured MTB cocci were maintained are: horizontal component = 0.18 Oe, vertical component = − 0.15 Oe, total intensity = 0.23 Oe.

To isolate the magnetic microorganisms for the experiments, a sub-sample was transferred to a specially designed flask containing a lateral capillary aperture and a small magnet generates a magnetic field aligned to the capillary aperture [12]. The studied “*Ca. M. multicellularis*” and uncultured MTB cocci are South-seeking and swam towards the capillary facing the North pole of a magnet. After some time, samples were collected with a micropipette.

To observe the magnetosome chains in the uncultured MTB cocci, a water drop containing cells, that were magnetically isolated, was transferred to formvar/carbon-coated copper grids and observed by transmission electron microscopy (Tecnai Spirit, FEI Company). For scanning electron microscopy, samples of sediment and water with “*Ca. M. multicellularis*” microorganisms were magnetically enriched using a neodymium iron boron magnet prior to fixation in glutaraldehyde 2.5% in sodium cacodylate buffer 0.1 M (pH 7.2; overnight at 4 °C). Samples were washed in the same buffer and post-fixed in osmium tetroxide 1% in sodium cacodylate buffer 0.1 M (pH 7.2) for 1 h at room temperature. After washing the samples again, ethanol series dehydration and CO₂ critical point drying were performed. Samples were sputtered with gold and observed in a JEOL JSM5310 scanning electron microscope operating at 15 kV.

U-turn trajectories were recorded to estimate the velocity and magnetic moment of “*Ca. M. multicellularis*” and of the uncultured MTB cocci. From the initial branch of the curve, the following trajectory parameters were calculated, assuming that the trajectory is a helix [5, 6, 9, 10]: the axial velocity, the trajectory frequency and radius. The U-turn method was used to estimate the magnetic moment for the magnetotactic microorganisms through the U-turn diameter D_U [13] because the recording rate was not proper to measure the U-turn time for higher magnetic fields in the uncultured MTB cocci. On the stage of an inverted microscope (Nikon Eclipse TS100) was set a pair of coils connected to a DC power supply and fixed

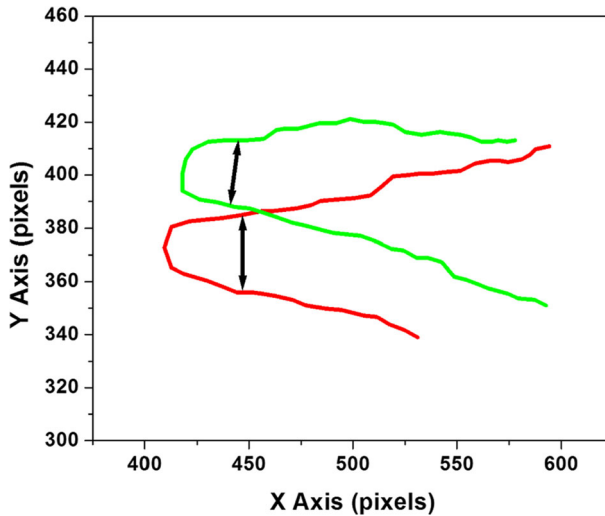


Fig. 1 Example of U-turn trajectory for two different uncultured MTB cocci. The double-head arrow shows the U-turn diameter D_U . Coordinates are in pixel units because are raw data. The curves were obtained in the presence of a magnetic field of 2 Oe. The drop border is located to the right of the figure, near to line $x = 600$ pixel

to a glass microscope slide where the collected drop with magnetotactic microorganisms was placed. The lens used had magnification of 40X for uncultured MTB cocci and 20X for “*Ca. M. multicellularis*” allowing the measurement of the microorganism radius R . The magnetic fields generated by the coils were 2 Oe, 4 Oe, 6 Oe, 8 Oe, 10 Oe and 15 Oe. An electric circuit for changing the voltage polarity (reversal of current) was connected between the power supply and coils, leading to the inversion of the magnetic field direction when the button was turned in on or off. After two magnetic field inversions, the magnetotactic microorganisms perform U-turn trajectories. The magnetic moment m can be estimated using the following equation for spherical magnetotactic microorganisms [13]:

$$D_U = 8\pi^2 \eta R^3 v / (mB) \quad (3)$$

where η is the water viscosity (10^{-3} Pa s), R is the microorganism radius, v is the velocity and B is the magnetic field.

To calculate D_U , the following procedure was performed: U-turn trajectories were recorded, in a frame rate of 82 fps, in the inverted microscope with a digital camera (Lumera Infinity 1). The coordinates of the U-turn trajectories were obtained using the software *ImageJ* (NIH—USA). The coordinates were in pixel units, and the conversion to μm was done using a calibration ruler, which consists in a 1 mm line divided in 100 parts. In the experimental setup, the external magnetic field is applied in the x direction. The trajectories that showed a clear U form were chosen to measure the distance among both arms in the trajectory (Fig. 1).

The axial velocity was measured analyzing the movement before the magnetic field inversion, assuming that the trajectory is similar to a cylindrical helix. In this case, if the helix axis is aligned to the magnetic field direction (X axis), then the coordinates in the XY plane must have the following parametrization:

$$x'(t) = V_{ax} \cdot t \quad (4a)$$

$$y'(t) = r \cdot \cos(2\pi ft + \phi_0) \tag{4b}$$

where V_{ax} is the axial velocity, r is helix radius, f is the helix frequency and ϕ_0 is a phase constant. In the case that the trajectory is not aligned to the magnetic field but inclined by an angle θ the coordinates must have the following expressions:

$$x(t) = x' \cos \theta + y' \sin \theta = r \cdot \sin \theta \cdot \cos(2\pi ft + \phi_0) + V_{ax} \cdot t \cdot \cos \theta \tag{5a}$$

$$y(t) = -x' \sin \theta + y' \cos \theta = r \cdot \cos \theta \cdot \cos(2\pi ft + \phi_0) - V_{ax} \cdot t \cdot \sin \theta. \tag{5b}$$

The coordinates $x(t)$ and $y(t)$ must be oscillating functions with linear tendencies. If θ is near to 0° then $x(t)$ must be similar to straight line and $y(t)$ must be an oscillating function with an inclination. The inclinations of $x(t)$ and $y(t)$ correspond to V_x and V_y , respectively, and $V_{ax} = (V_x^2 + V_y^2)^{1/2}$. The analysis of $y(t)$ permits the calculation of $r \cdot \cos \theta$ and f .

2.1 Kinetic energy for “*Ca. M. multicellularis*”

As shown by Eq. 1, the kinetic energy has translational and rotational contributions. The translational kinetic energy depends on the trajectory velocity that is calculated as

$$V_{Trans} = (V_{ax}^2 + 4\pi^2 r^2 f^2)^{1/2} \tag{6}$$

where V_{ax} is the axial velocity, r is the trajectory radius and f is the trajectory frequency. The body rotation frequency must be measured in order to calculate the rotational kinetic energy $0.5 \cdot I_{cm} \omega^2$. As shown by Keim et al. [14], “*Ca. M. multicellularis*” rotates its body with a frequency equal to the trajectory frequency. The moment of inertia I_{cm} is $0.4MR^2$ for a spherical body, where M is the mass and R the radius of the body. Finally, the total kinetic energy E_K can be written as:

$$K_{CMM} = 0.5M(V_{ax}^2 + (r^2 + 0.4R^2)4\pi^2 f^2). \tag{7}$$

2.2 Kinetic energy for the uncultured MTB cocci

In the case of the uncultured MTB cocci, it is not easy to determine the body rotation frequency from the trajectory. The recording rate of 82 fps permits to measure frequencies up to 41 Hz, and the body rotates at frequencies of about 100 Hz [15]. So, in the present study it was only possible the estimative of the translational kinetic energy. As shown by Acosta-Avalos and Rodrigues [9], the bacterial trajectory is composed by two helices. In that case, the translational kinetic energy can be written approximately as:

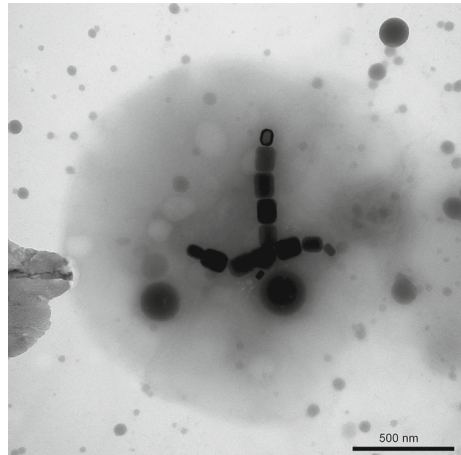
$$K_{MTB} = 0.5M(V_{ax}^2 + 4\pi^2 r_1^2 f_1^2 + 4\pi^2 r_2^2 f_2^2) \tag{8}$$

where r_i and f_i are the radius and the frequency for the helix i (1 or 2).

The other dynamical parameters as the flagellar force F_{Fla} and flagellar output power P_{Fla} are explained below.

All graphics and analysis were done using the software *Microcal Origin* and the statistics with the software *GraphPad InStat*.

Fig. 2 Transmission electron microscopy image of magnetotactic cocci from Rodrigo de Freitas Lagoon, Rio de Janeiro, Brazil. Note the presence of two chains of magnetosomes. Bar = 500 nm



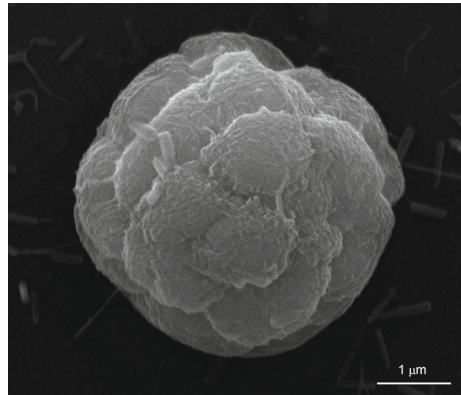
3 Results and discussion

3.1 Description of magnetosomes and magnetic moment of the microorganisms

The electron micrographs permit to describe the uncultured MTB cocci as spheroids with diameter $1.65 \mu\text{m} \pm 0.27 \mu\text{m}$ (mean \pm SD, $N = 23$ cocci) (Fig. 2). Each coccus has two chains with 7 ± 2 magnetosomes (mean \pm SD, $N = 46$ chains). Magnetosome images are similar to the bidimensional projections of elongated cuboctahedrons, commonly observed in magnetite magnetosomes [16]. Their dimensions are: length = $115 \text{ nm} \pm 26 \text{ nm}$ and width = $93 \text{ nm} \pm 24 \text{ nm}$, and the axial ratio (width/length) is 0.81 ± 0.08 (mean \pm SD, $N = 245$ magnetosomes). Those dimensions correspond well with single domain nanoparticles of magnetite. Considering each magnetite nanoparticle as a parallelepiped, it is possible to calculate its magnetic moment as $V \cdot M_V$, where V is the nanoparticle volume and M_V is the magnetic moment per unit volume of magnetite ($0.48 \text{ Am}^2/\text{cm}^3$). The magnetic moment for each magnetosome is $(5.5 \pm 2.9) \times 10^{-16} \text{ Am}^2$ (mean \pm SD, $N = 245$ magnetosomes). Considering that all magnetosomes in the chain have their magnetic moments parallel, each chain must have a magnetic moment = $(4.04 \pm 1.78) \times 10^{-15} \text{ Am}^2$ (mean \pm SD, $N = 46$ chains) and each bacterium must have a magnetic moment of $(7.98 \pm 3.57) \times 10^{-15} \text{ Am}^2$ (mean \pm SD, $N = 23$ bacteria). This description is more complete than that description done by Acosta-Avalos et al. [17] where are described the statistics for only 7 bacteria.

“*Ca. M. multicellularis*” is a spherical multicellular magnetotactic prokaryote (Figure 3) with 6 to 9 μm in diameter and composed of 10 to 40 Gram negative MTB [18]. A description of the magnetosome distribution and magnetic moment in the whole body in “*Ca. M. multicellularis*” is difficult to do, because of the complex spatial distribution of the magnetosomes in its volume. In a spatial reconstruction study done using serial ultrafine cuts in “*Ca. M. multicellularis*” [19], it was possible to analyze the distribution of magnetosomes around the spherical body of “*Ca. M. multicellularis*”. Silva [19] observed that each “*Ca. M. multicellularis*” is composed in average by 17 MTB. Each MTB biomineralize nanoparticles of greigite (Fe_3S_4) and presents 6 ± 2 (mean \pm SD) magnetosome chains and each chain has 9 ± 2 (mean \pm SD) magnetosomes. In average, each magnetosome has length = $83 \text{ nm} \pm 10 \text{ nm}$ (mean \pm SD) and axial ratio of about 0.78. That permits to estimate the magnetosome width as about 65 nm. Following the same procedure described above to estimate the magnetic

Fig. 3 Scanning electron microscopy of the multicellular magnetotactic prokaryote “*Ca. M. multicellularis*.” Note that the spherical microorganism is composed of several cells



moment in each MTB composing “*Ca. M. multicellularis*,” it is assumed that the magnetic moments of the magnetosomes composing each chain are parallel and that the magnetic moments of the chains are also parallel. For each magnetosome, its magnetic moment is estimated as $V \cdot M_V$, where V is the magnetosome volume and M_V is the magnetic moment per unit volume of greigite ($0.123 \text{ Am}^2/\text{cm}^3$) [20, 21]. Assuming that each magnetosome is a parallelepiped, then its average magnetic moment must be $0.43 \times 10^{-16} \text{ Am}^2$. Each chain must have a magnetic moment of about $3.9 \times 10^{-16} \text{ Am}^2$ and each MTB composing “*Ca. M. multicellularis*” must present a magnetic moment of about $2.3 \times 10^{-15} \text{ Am}^2$. As Winklhofer et al. [22] and Acosta-Avalos et al. [23] showed, “*Ca. M. multicellularis*” presents a degree of magnetic optimization of about 0.85 and defined as the magnetic moment of the microorganism divided by the maximum magnetic moment that the microorganism can have. If “*Ca. M. multicellularis*” is compound in average by 17 MTB [24], then the maximum magnetic moment it can have is $39 \times 10^{-15} \text{ Am}^2$ (considering that all magnetic moments are parallel). The actual value considering the degree of magnetic optimization must be $33 \times 10^{-15} \text{ Am}^2$. In the analysis below, we must use that value as the expected average magnetic moment for “*Ca. M. multicellularis*”.

3.2 Trajectory parameters as function of the magnetic field

Table 1 shows the resulting parameters for the trajectories for each microorganism. The velocity values for the uncultured cocci are in accord with the values reported for the same uncultured MTB cocci by Acosta-Avalos et al. [17] ($85.6 \mu\text{m/s}$ at 2.8 Oe) and De Melo et al. [10] ($89 \mu\text{m/s}$ at 0.7 Oe). Figure 4 shows V_{ax} as a function of the magnetic field. A similar behavior has been estimated theoretically by Acosta-Avalos and Rodrigues [9] through a dynamical model for the motion of a spherical MTB with only a flagellum. They assumed that the flagellum produce an oscillating force on the MTB surface described as:

$$\mathbf{F}_f = F_{12}(\cos(\omega_f t)\mathbf{i} + \sin(\omega_f t)\mathbf{j}) + F_3\mathbf{k} \quad (9)$$

where \mathbf{k} is a versor perpendicular to the surface and versors \mathbf{i} and \mathbf{j} are in a tangent plane to the contact point. Acosta-Avalos and Rodrigues [9] showed that when $F_3 = 100 F_{12}$, the velocity shows a minimum at about 5 Oe. In Fig. 4, V_{ax} for the uncultured MTB shows a minimum at about 5 Oe. However, the MTB magnetic moment used in the numerical simulation is $1.5 \times 10^{-15} \text{ Am}^2$ which is lower than the magnetic moment estimated for the uncultured MTB cocci by electron microscopy: $7.98 \times 10^{-15} \text{ Am}^2$. The relation among F_{12} and F_3 must be

Table 1 Kinematic parameters of the trajectories as a function of the magnetic field B for the uncultured MTB cocci and “*Ca. M. multicellularis*”: axial velocity V_{ax} , radius r_1 and frequency f_1 of the first helical component and radius r_2 and frequency f_2 of the second helical component only for the uncultured MTB cocci

B (Oe)	V_{ax} ($\mu\text{m/s}$)	r_1 (μm)	f_1 (Hz)	r_2 (μm)	f_2 (Hz)	R (μm)	N
Uncultured MTB cocci							
2.3	87 ± 13^{AB}	0.37 ± 0.22^{AB}	4.1 ± 1.9^{AB}	0.17 ± 0.12^A	19 ± 9^A	0.71 ± 0.08	50
4	84 ± 12^{ABC}	0.45 ± 0.26^A	2.4 ± 1.6^C	0.16 ± 0.17^{AB}	16 ± 6^{AB}	0.76 ± 0.09	50
5.2	81 ± 13^{BC}	0.44 ± 0.26^A	2.8 ± 1.8^{CB}	0.15 ± 0.11^A	14 ± 4^B	0.75 ± 0.07	50
7.6	83 ± 12^{ABC}	0.29 ± 0.18^B	3.5 ± 2.2^B	0.14 ± 0.12^{AB}	15 ± 6^B	0.74 ± 0.11	50
9.7	89 ± 12^A	0.32 ± 0.16^B	2.9 ± 1.8^{CB}	0.11 ± 0.05^B	15 ± 6^B	0.70 ± 0.07	50
15	77 ± 10^C	0.34 ± 0.19^{AB}	3.3 ± 2.4^{CB}	0.09 ± 0.03^B	14 ± 4^B	0.70 ± 0.07	50
“ <i>Ca. M. multicellularis</i> ”							
2	97 ± 18^A	2.6 ± 1.3^A	1.7 ± 0.7^A	–	–	2.8 ± 0.4	50
4	100 ± 24^A	2.7 ± 1.7^A	1.6 ± 0.8^A	–	–	2.7 ± 0.4	50
6	116 ± 22^B	2.5 ± 1.4^A	1.7 ± 0.5^A	–	–	2.8 ± 0.3	50
8	116 ± 17^B	2.2 ± 1.2^A	1.6 ± 0.6^A	–	–	2.9 ± 0.4	50
10	107 ± 26^A	2.3 ± 1.3^A	1.4 ± 0.8^A	–	–	2.9 ± 0.3	50
15	127 ± 26^B	1.9 ± 1.3^A	1.7 ± 0.7^A	–	–	2.9 ± 0.3	50

It is shown also the radius R of the microorganisms. N is the number of trajectories analyzed. Data are reported as Mean \pm Standard Deviation. Letters in the columns represent the statistical similarity or difference (ANOVA TEST, $p < 0.05$): equal letters means statistical similarity

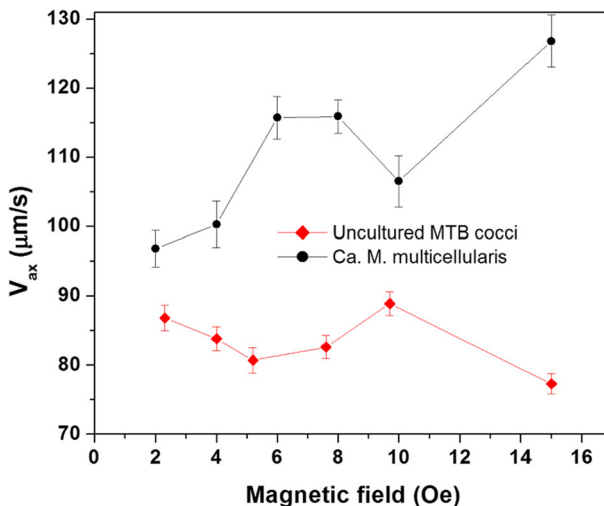


Fig. 4 Mean axial velocity V_{ax} as a function of the magnetic field for the uncultured MTB cocci and “*Ca. M. multicellularis*.” Bars in the symbols represent the standard error

different than 100 but must prevail the relation $F_3 \gg F_{12}$. The same was not observed for V_{ax} of “*Ca. M. multicellularis*,” where an oscillation among two values was seen. Qualitatively, r and f for the uncultured MTB cocci follow a similar behavior as predicted by the theoretical

model: an increase and later decrease for r and a decrease in f (Figs. 4 and 5 in [9]). For “*Ca. M. multicellularis*,” the same was not observed, and r had a tendency to decrease (ANOVA test $p \approx 0.05$) and f maintained almost the same values for all the magnetic fields studied. The microorganism size R measured by optical microscopy was in the same range as has been reported by others and in good agreement with electron microscopy measurements: about $0.74 \mu\text{m}$ for the uncultured MTB cocci [17] and about $2.8 \mu\text{m}$ for “*Ca. M. multicellularis*” [25]. The trajectory parameters observed for the uncultured MTB cocci as a function of the magnetic field could be well explained by the theoretical model of motion for a spherical MTB with one flagellum [9, 26]. For “*Ca. M. multicellularis*,” there is no model to explain its motion, once it is composed by several MTB, each with several short flagella distributed around the body of “*Ca. M. multicellularis*” [27]. It is interesting to observe that the model for MTB motion predicts that a flagellar rotation of 40 Hz produces frequency trajectories from about 36 Hz to 27 Hz [9]. If the flagellar rotation is higher than 40 Hz the trajectory frequencies must be higher. Recently, Bente et al. [28] showed that MTB present trajectories with two frequencies at about 13 Hz and 80 Hz. Lowe et al. [15] showed that motile *Streptococcus* presented two frequencies in their trajectories. One lower at about 7 Hz associated with the roll of the bacterial body (as a counter-rotation to the flagellar bundle rotation) and another higher at about 90 Hz associated with the wobble or funnel movement of the bacterial body and related to the vibration of the cell body at the frequency of the flagellar rotation [15]. The model for MTB motion described by Acosta-Avalos and Rodrigues [9] assumes a spherical bacterium with a single flagellum collinear to the bacterium body diameter. The frequency f_1 (Table 1) observed in the trajectory of the uncultured MTB cocci has been reported by De Melo et al. [10] for the same uncultured MTB cocci and by Acosta-Avalos and Rodrigues [9] for other uncultured cocci and must be associated with the body rolling according to Lowe et al. [15]. The presence of that lower frequency f_1 cannot be explained by the motion models for MTB [9], and efforts must be done in those models to analyze the bacterial trajectories in real conditions. In the other hand, in our experimental setup the frame rate of 82 fps permitted the observation of frequencies only up to 40 Hz. Future experiments in our laboratory with frame rates of 180 fps will be done to observe that higher trajectory frequencies.

3.3 Trajectory orientation and the paramagnetic model

Table 2 shows the statistics for $\cos\theta$ from the set of angles θ between the trajectory direction and the magnetic field. An organism that swims along a helical trajectory has the axis of the helix as the direction of motion [29]. The axial velocity is directed along the helical axis, and the magnetic field was directed along the x axis in our experimental setup, allowing the measurement of the angle θ as the angle between the axial velocity V_{ax} and the x axis. Kalmijn [3] describes the Paramagnetic model for magnetotactic bacteria, assuming that a tiny bacterium with a magnetic moment can be considered as a paramagnet influenced by the thermal energy $k_B T$, being randomly disoriented from the magnetic field direction. This idea permits the use of the Boltzmann statistics to calculate the average value of $\cos\theta$ ($\langle \cos\theta \rangle$), being considered as an estimator of the efficiency of the magnetotactic trajectory orientation, and its variance σ^2 . Kalmijn [3] shows that:

$$\langle \cos\theta \rangle = \coth(X) - 1/X \quad (10a)$$

$$\sigma^2 = 1 - \coth^2(X) + 1/X^2 \quad (10b)$$

where X is the ratio between the magnetic energy and the thermal energy: $X = (mB/k_B T)$, where m is the magnetic moment of the microorganism, B is the magnetic field, k_B is the

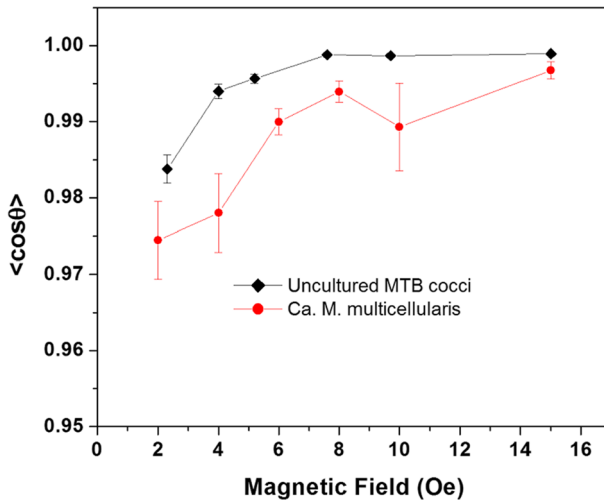


Fig. 5 Average value of $\cos\theta$ ($\langle\cos\theta\rangle$) as a function of the magnetic field for the uncultured MTB cocci and “*Ca. M. multicellularis*.” Bars in the symbols represent the standard error. Line is only a guide to the eyes

Boltzmann constant and T is the absolute temperature. It has been assumed that the analysis of $\langle\cos\theta\rangle$ as a function of B permits the measurement of the magnetic moment of magnetotactic bacteria [3]. Figure 5 shows $\langle\cos\theta\rangle$ as a function of B for the uncultured MTB cocci and “*Ca. M. multicellularis*.” It was observed that at lower magnetic fields the magnetotactic orientation efficiency is better for the uncultured MTB cocci than for “*Ca. M. multicellularis*.” A fit of $\langle\cos\theta\rangle$ to a Langevin curve (Eq. 10a) in Fig. 5 permitted the estimation of $(m/k_B T)$. For uncultured MTB cocci: $(m/k_B T) \approx 32.9$ and for “*Ca. M. multicellularis*”: $(m/k_B T) \approx 16.8$. Assuming the temperature as 300 K, the estimated magnetic moment is about $1.3 \times 10^{-15} \text{ Am}^2$ for the uncultured MTB cocci and $0.7 \times 10^{-15} \text{ Am}^2$ for “*Ca. M. multicellularis*.” According to Acosta-Avalos et al. [17], these uncultured MTB cocci have a magnetic moment distribution, measured through the U-turn method that shows a maximum at about $1.4 \times 10^{-15} \text{ Am}^2$ (Online Resource 1). The value calculated from the Langevin function fit is in accord with the maximum of the distribution but is lower than the average value calculated directly from the magnetosome chains: $7.9 \times 10^{-15} \text{ Am}^2$. That difference (Transmission electron microscopy estimates greater than estimates using the Paramagnetic model) has been observed by others [30, 31] and has been attributed to non-thermal perturbations created by the flagellar movement [3, 32], being quantified through an effective temperature T_{Eff} higher than the ambient temperature. The magnetic moment estimated for “*Ca. M. multicellularis*” was much lower than the value estimated for these organisms using the U-turn technique [33], of about $10 \times 10^{-15} \text{ Am}^2$, and much lower than the theoretical value estimated from the magnetosome chains of about $33 \times 10^{-15} \text{ Am}^2$. The first conclusion is that the Paramagnetic model applies well to the uncultured MTB cocci but not to the complex microorganism as “*Ca. M. multicellularis*.” “*Ca. M. multicellularis*” is composed in average by 17 flagellated MTB, and these flagella do not form bundles. Therefore, “*Ca. M. multicellularis*” must move through the coordinated movement of the flagella of each MTB. The paramagnetic model assumes that the magnetic orientation of a single MTB can be perturbed thermally. To apply that model to “*Ca. M. multicellularis*,” it must be considered that each MTB composing it is trying to orient itself to the magnetic field and also that each MTB is attached to a structure

Table 2 Statistics for the paramagnetic model

B (Oe)	$\langle \cos\theta \rangle$	σ^2	X	$\langle m \rangle \times 10^{-15}$ (Am ²)	T_{Eff} (K)
Uncultured MTB cocci					
2.3	0.98378	1.7522×10^{-4}	61.5	1.1	1860
4	0.99401	4.56649×10^{-4}	173	1.8	1369
5.2	0.99568	1.86832×10^{-5}	231.5	1.8	1235
7.6	0.9988	2.53276×10^{-6}	833.7	4.5	480
9.7	0.99867	1.75884×10^{-6}	751.9	3.2	684
15	0.99894	1.31443×10^{-6}	943.5	2.6	909
"Ca. M. multicellularis"					
2	0.97444	1.27×10^{-3}	39.6	0.81	12×10^3
4	0.97801	1.34×10^{-3}	46.4	0.48	21×10^3
6	0.98998	1.46371×10^{-4}	100	0.68	14×10^3
8	0.99395	9.70502×10^{-5}	166.1	0.85	12×10^3
10	0.98930	1.65×10^{-3}	100.8	0.41	24×10^3
15	0.99674	6.61115×10^{-5}	309.4	0.85	12×10^3

The average $\cos\theta$ ($\langle \cos\theta \rangle$) and its variance σ^2 are used to calculate the ratio X between the magnetic energy mB and the thermal energy $k_B T$ through Eq. (11). From the values of X , it is possible to estimate the average magnetic moment $\langle m \rangle$ assuming a temperature of 300 K (ambient temperature) or to estimate the effective temperature T_{Eff} assuming for the microorganism magnetic moment the values obtained from electron micrographs: 7.9×10^{-15} Am² for the uncultured MTB cocci and 33×10^{-15} Am² for "Ca. M. multicellularis." Data are reported as Mean \pm Standard Deviation

with several MTB positioned at constant relative positions, as a rigid body. When one MTB tries to orient itself to the magnetic field at the same time, it disorients the other MTB in the microorganism. That produces a higher disorientation in every MTB composing "Ca. M. multicellularis," and also in the whole microorganism, producing the inferior results observed in the present manuscript.

Acosta-Avalos et al. [17] showed that it is possible to estimate the energy ratio X for each magnetic field value, combining Eqs. 10a and 10b:

$$X = (2* \langle \cos\theta \rangle) / (1 - \langle \cos\theta \rangle^2 - \sigma^2). \quad (11)$$

Table 2 shows the values of X for the uncultured MTB cocci and for "Ca. M. multicellularis." Using those values, the average value of the microorganism magnetic moment $\langle m \rangle$ (assuming $T = 300$ K) and the effective temperature T_{Eff} (assuming $m = 7.9 \times 10^{-15}$ Am² for the uncultured MTB cocci and 33×10^{-15} Am² for "Ca. M. multicellularis") were calculated. It was observed that the non-thermal perturbation decreases after 5 Oe producing better magnetic moment estimates for the uncultured MTB cocci. That change is like a step: before 5 Oe the flagellar perturbations were turned in on and after 5 Oe they were turned in off. For "Ca. M. multicellularis," the non-thermal perturbation was almost constant, with a value at about 1.5×10^4 K. The behavior observed for the uncultured MTB cocci has been observed also in *Magnetospirillum magneticum* strain AMB-1 [34], where it was observed that AMB-1 cells are able to sense the angle among the magnetic moment and the magnetic field through some proteins linked from the cytoskeleton to the flagella, determining an active magnetic field sensing. That active sensing had strong influence for lower magnetic fields

(<50 Oe) and is ignorable for higher magnetic fields (> 50 Oe), where passive magnetotaxis is dominant. For “*Ca. M. multicellularis*,” the same was not observed and the non-thermal perturbation was maintained for all the magnetic fields analyzed.

3.4 U-turn diameter and drag coefficient

The U-turn technique has been commonly used to estimate the magnetic moment of magnetotactic microorganisms [13] but can also be used to analyze other features of the motility dynamics in MTB [8]. Table 3 shows the U-turn diameter D_U as a function of the magnetic field for the uncultured MTB cocci and for “*Ca. M. multicellularis*”. For “*Ca. M. multicellularis*,” D_U was almost ten times the value for the uncultured MTB cocci. The values of D_U decrease with the magnetic field as expected from Eq. (3). The simple analysis for the U-turn technique assumes that the total torque is null [13], and that the drag torque T_D is proportional to the angular velocity ($T_D = f_V \omega$), meaning that:

$$T_{\text{mag}} + T_D = mB \sin \delta - f_V(d\delta/dt) = 0 \quad (12)$$

where δ is the angle between the magnetic moment and the magnetic field during the U-turn. Solving the differential Eq. (12), it is possible to show that $D_U = \pi f_V V_{\text{ax}}/mB$ [13]. The parameter V_{ax}/D_U (rad/s) can be interpreted as an average rate of rotation [8] and can be written as:

$$V_{\text{ax}}/D_U = \gamma B \quad (13)$$

where $\gamma = m/\pi f_V$. Assuming that the magnetic moment m is the average value observed in the micrographs of magnetosome chains, it is possible to estimate the rotational drag coefficient f_V . Table 3 and Fig. 4 show V_{ax}/D_U as a function of the magnetic field. It was observed that there is a linear relation among both parameters as expected from Eq. (13). Assuming that when $B = 0$, the rate $V_{\text{ax}}/D_U \rightarrow 0$, the linear fit in Fig. 3 produces the following values for γ : 3.9 ± 0.7 (rad/Oe·s) for the uncultured MTB cocci and 0.46 ± 0.05 (rad/Oe s) for “*Ca. M. multicellularis*.” For *Magnetospirillum gryphiswaldense* strain MSR-1, a value of $\gamma = 0.074$ (rad/Oe·s) has been measured [8]. The difference among the values obtained here could be related to the geometrical form and size of MSR-1 cells that is a thin spiral, in contrast with the uncultured MTB cocci and “*Ca. M. multicellularis*” that are spheres. Assuming that the magnetic moment for the uncultured MTB cocci and “*Ca. M. multicellularis*” is, respectively, 7.9×10^{-15} Am² and 33×10^{-15} Am², the respective experimental values for the rotational drag coefficient f_V are 64×10^{-21} (N m s) and 23×10^{-19} (N m s). The theoretical value for f_V using the expression for spherical bodies ($f_V = 8\pi\eta R^3$) and using the values of R in Table 1 (≈ 0.73 μm and ≈ 2.8 μm for the uncultured MTB cocci and for “*Ca. M. multicellularis*,” respectively) produce the values 9.8×10^{-21} (N m s) for the uncultured MTB cocci and 5.5×10^{-19} (N m s) for “*Ca. M. multicellularis*.” The difference between the theoretical and experimental values can be understood through an effective radius R_{Eff} to calculate the drag coefficient. For the uncultured MTB cocci, the experimental value $f_V = 64 \times 10^{-21}$ (N m s) resulted in a value of $R_{\text{Eff}} \approx 1.4$ μm and for “*Ca. M. multicellularis*,” the experimental value $f_V = 23 \times 10^{-19}$ (N m s) produced a value of $R_{\text{Eff}} \approx 4.5$ μm . Those values of R_{Eff} are similar to the values of the sum of R plus the trajectory radius, meaning that the rotation drag coefficient is related to some “effective radius” of the microorganism moving in a helical trajectory. Table 3 displays the calculation of the magnetic moment as a function of the magnetic field, assuming the geometrical expression for f_V . It was observed that the values were similar for all the magnetic fields, as expected. For the uncultured MTB cocci, the values were similar to those reported by Acosta-Avalos et al. [17] and for “*Ca. M. multicellularis*”

Table 3 Statistics for U-turn parameters as a function of the magnetic field B

B (Oe)	D_U (μm)	V_{ax}/D_U (rad/s)	$m \times 10^{-15}$ (Am^2)	N
Uncultured MTB cocci				
2.3	6.4 ± 2.1	14.5 ± 6.1	1.8 ± 1.0	36
4	4.9 ± 1.8	17.6 ± 5.1	1.5 ± 0.5	37
5.2	4.5 ± 1.3	19.6 ± 7.1	1.2 ± 0.4	30
7.6	3.6 ± 1.8	29.8 ± 15.5	1.4 ± 1.0	30
9.7	2.0 ± 0.9	56.5 ± 28.1	1.5 ± 0.8	29
15	1.9 ± 1.4	55.1 ± 40.2	1.0 ± 0.7	29
"Ca. M. multicellularis"				
2	44.7 ± 16.6	2.5 ± 0.9	23.7 ± 13.1	36
4	38.7 ± 13.8	3.0 ± 1.3	16.2 ± 13.4	33
6	36.3 ± 14.9	4.0 ± 2.5	12.3 ± 10.6	37
8	31.3 ± 15.6	4.4 ± 1.9	11.2 ± 5.2	32
10	24.8 ± 9.9	5.0 ± 1.9	10.0 ± 4.5	31
15	20.1 ± 8.8	7.9 ± 6.2	11.5 ± 11.3	32

The U-turn diameter D_U is used to calculate the individual magnetic moment using Eq. (3), and the average magnetic moment m is also calculated. The parameter V_{ax}/D_U is used to calculate the proportionality coefficient $\gamma = m/\pi f_V$ as shown in Fig. 6. N is the number of U-turns analyzed. Data are reported as Mean \pm Standard Deviation

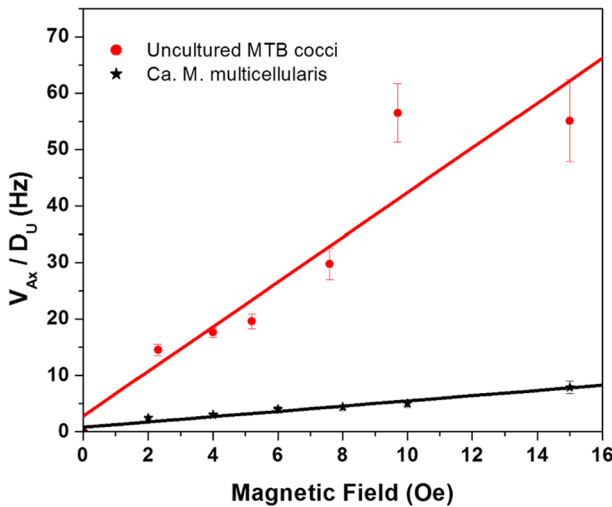


Fig. 6 V_{ax}/D_U as a function of the magnetic field for the uncultured MTB cocci and "Ca. M. multicellularis." Bars in the symbols represent the standard error. It is observed that V_{ax}/D_U increases linearly with the magnetic field. Solid lines are the linear fit to corresponding data, and the corresponding angular coefficients are 3.9 ± 0.7 (rad/Oe s) for the uncultured MTB cocci and 0.46 ± 0.05 (rad/Oe s) for "Ca. M. multicellularis"

the values were similar to those reported by Perantoni et al. [33] and De Melo and Acosta-Avalos [25]. These values are necessary to calculate the magnetic energy in the following section.

3.5 Kinetic energy, flagellar force and flagellar power

Table 4 shows the dynamical parameters obtained from the bacterial trajectories: the magnetic energy E_{Mag} calculated as $m \cdot B \cdot \cos\theta$, assuming that the magnetic moment has the same direction as the trajectory, the kinetic energy K calculated as described above and the flagellar

Table 4 Dynamical parameters obtained from the motion trajectories as a function of the magnetic field B for the uncultured MTB cocci and “*Ca. M. multicellularis*”

B (Oe)	$E_{\text{Mag}} \times 10^{-19}$ (J)	$K \times 10^{-22}$ (J)	$K/k_{\text{B}}T \times 10^{-2}$	$P_{\text{Fla}} \times 10^{-16}$ (W)	$F_{\text{Fla}} \times 10^{-12}$ (N)
Uncultured MTB cocci					
2.3	4.1 ± 2.3	0.062 ± 0.025	0.17 ± 0.09	1.2 ± 0.5	1.1 ± 0.2
4	5.9 ± 2.0	0.075 ± 0.038	0.19 ± 0.1	1.1 ± 0.3	1.2 ± 0.2
5.2	6.2 ± 2.0	0.063 ± 0.026	0.16 ± 0.08	1.0 ± 0.5	1.1 ± 0.2
7.6	8.2 ± 5.5	0.064 ± 0.027	0.17 ± 0.08	1.0 ± 0.3	1.1 ± 0.2
9.7	10.9 ± 5.6	0.062 ± 0.026	0.15 ± 0.06	1.1 ± 0.4	1.2 ± 0.2
15	13.1 ± 7.1	0.045 ± 0.018	0.11 ± 0.04	0.8 ± 0.2	1.0 ± 0.2
“ <i>Ca. M. multicellularis</i> ”					
2	43.8 ± 22.3	5.9 ± 3.7	14 ± 9	5.8 ± 2.4	5.2 ± 1.2
4	46.8 ± 27.2	6.2 ± 4.4	15 ± 10	6.2 ± 2.9	5.3 ± 1.8
6	60.4 ± 30.1	7.5 ± 4.7	18 ± 10	7.8 ± 3.3	6.1 ± 1.5
8	89.2 ± 41.6	8.7 ± 4.5	21 ± 10	8.0 ± 2.7	6.5 ± 1.4
10	98.7 ± 44.6	6.8 ± 3.7	16 ± 10	6.8 ± 3.1	5.8 ± 1.6
15	134.7 ± 61.9	11.2 ± 7.3	27 ± 20	10.0 ± 4.8	7.2 ± 2.1

The magnetic energy E_{Mag} was estimated using the values of magnetic moment calculated with the U-turn diameter. The kinetic energy K and its value relative to the thermal energy $k_{\text{B}}T$, the flagellar force F_{Fla} and the flagellar output power P_{Fla} are explained in the text. Data are reported as Mean \pm Standard Deviation

power P_{Fla} calculated as: $F_{\text{Drag}} \cdot V_{\text{ax}} = 6\pi\eta R V_{\text{ax}}^2$. It was observed that for the uncultured MTB cocci the kinetic energy and flagellar power were almost constant, with values at about 6.2×10^{-24} J and 1×10^{-16} W, respectively. However, for “*Ca. M. multicellularis*,” the kinetic energy and flagellar power increased almost linearly as a function of the magnetic energy or the magnetic field intensity (Table 4 and Fig. 7).

It was observed that the kinetic energy was lower than the disorienting thermal energy $k_{\text{B}}T = 4.14 \times 10^{-21}$ J at 300 K. For the uncultured MTB cocci, the ratio is $K/k_{\text{B}}T \approx 0.0016$ and for “*Ca. M. multicellularis*” it increased from 0.14 to 0.27. Those $K/k_{\text{B}}T$ ratios are very small, because it is hoped that that ratio be higher than 1. Marshall et al. [35] estimated the kinetic energy of the monotrichous rod-shaped bacteria *Pseudomonas* R3 at about 5.45×10^{-25} J. That value is about 10 times lower than the kinetic energy for the uncultured MTB cocci because the maximum velocity of *Pseudomonas* R3 was $33 \mu\text{m/s}$, a value lower than the minimum average velocity ($77 \mu\text{m/s}$) measured in the uncultured MTB cocci. However, in *Escherichia coli* bacteria, optical trapping techniques permitted to estimate the kinetic energy of those bacteria in the range between 678 and $2063 k_{\text{B}}T$ [36]. The very small ratios obtained for the uncultured MTB cocci and “*Ca. M. multicellularis*” in the present manuscript can be understood considering that the trajectory was obtained following the center of the body. A bacterium is a compound object, having a body and flagella. Thus, the total kinetic energy is composed by the sum of the body kinetic energy and the flagellar kinetic energy. The kinetic energy measured using the trajectory data corresponds to the body kinetic energy. As has been assumed for other bacteria, $K/k_{\text{B}}T$ must be higher than 1 to the maintenance of bacterial direction in long paths. From our results, it can be inferred that the main contribution for the MTB total kinetic energy comes from the flagella. However, until the present moment there is no information about the flagella of the uncultured MTB cocci. But we can assume that, as in other MTB cocci as *Magnetococcus marinus* strain MC-1 and *Candidatus Magnetococcus*

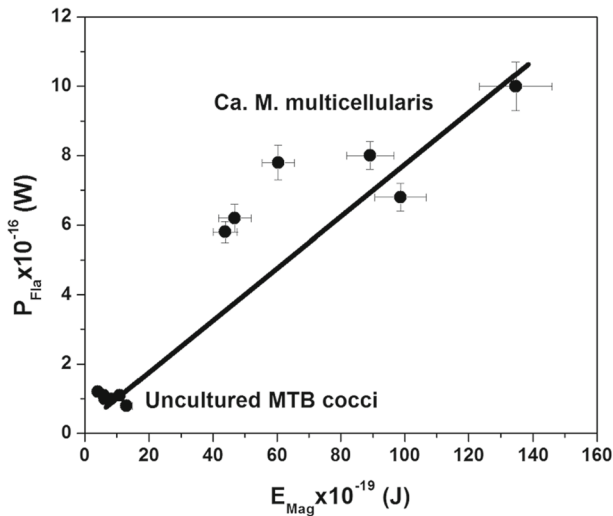


Fig. 7 Flagellar output Power (P_{Fla}) as a function of the magnetic energy (E_{Mag}) for the uncultured MTB cocci and “*Ca. M. multicellularis*.” Bars represent the standard error. The straight line is only a guide to the eyes. It is clearly observed that data for the uncultured MTB cocci form a cluster while for “*Ca. M. multicellularis*” the power P_{Fla} increases with the magnetic energy E_{Mag}

massalia strain MO-1, the uncultured MTB cocci must present a flagellar apparatus with two lophotrichous bundles. Considering the dimensions reported for the flagella of *Candidatus Magnetococcus massalia* strain MO-1 [37]: length = 2.5 μm , helix radius = 0.3 μm , flagellar diameter = 0.1 μm , and considering the protein mass density as 1.35 g/cm^3 , it is possible to estimate the contribution to the kinetic energy of both flagella, considering that they rotate at about 100 Hz [28] and that the flagellum moment of inertia is similar to $I = MR^2$, being M the flagellum mass and R the flagellar helix radius. The flagellar kinetic energy must be $2 \cdot (1/2 \cdot I \cdot \omega^2) = I \cdot \omega^2$. Using the values above, we obtain the following kinetic energy: 1.5×10^{-24} J that is similar to the average translation kinetic energy calculated in the present manuscript for the uncultured MTB cocci (6.2×10^{-24} J). This shows that the total kinetic energy for the uncultured MTB cocci is lower than $k_B T$. Even considering a flagellar rotation velocity of 1100 Hz (as estimated by Yang et al. [37]), the total kinetic energy continues to be lower than $k_B T$. Our conclusion is that the thermal energy is not disorienting the MTB trajectories because the magnetic torque produces an orientation that is more effective than the thermal disorientation, and for that reason the total kinetic energy does not need to be higher than $k_B T$.

In the amphitrichous (biflagellated) magnetotactic bacterium *M. magneticum* strain AMB-1 a magnetic trap made possible the measurement of the flagellar force F_{Flag} , and together with the cell velocity and the magnetic moment, using the U-turn technique, it was possible to estimate the power output of the flagellum P_{Fla} , that is an indicator of the availability and efficiency of consumption of energetic resources [11]. For *M. magneticum* strain AMB-1, Pierce et al. [11] were able to measure an average velocity of 18.3 $\mu\text{m}/\text{s}$ and average F_{Flag} of 29×10^{-15} N, producing an average power output of the flagellum $P_{Fla} \approx 0.5 \times 10^{-18}$ W (values amongst 0.2×10^{-18} W and 2×10^{-18} W). For the uncultured MTB cocci, using the average radius of 0.7 μm and a velocity of about 80 $\mu\text{m}/\text{s}$, a flagellar trust of about 1.1×10^{-12} N was obtained, and the power output of the flagellum was approximately 1×10^{-16} W.

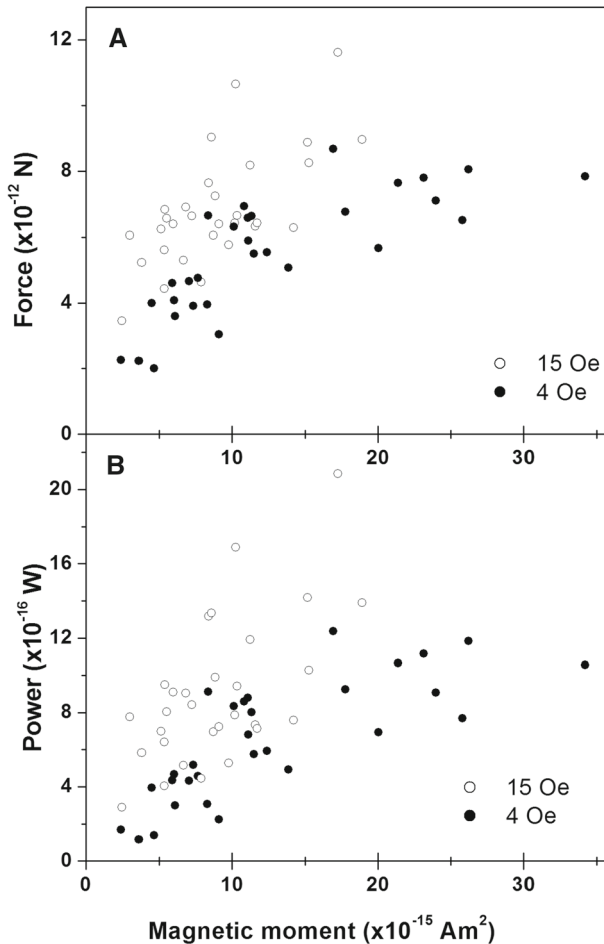


Fig. 8 a Flagellar force (F_{Fla}) as a function of the magnetic moment for “*Ca. M. multicellularis*” in two different magnetic fields. Solid symbols correspond to a magnetic field of 4 Oe and hollow symbols to a magnetic field of 15 Oe. It is clearly seen a positive correlation among both variables in both cases (Correlation coefficient $r = 0.78$ and significance $p < 0.0001$ for 4 Oe and $r = 0.67$ and significance $p < 0.0001$ for 15 Oe). **b** Flagellar output power (P_{Fla}) as a function of the magnetic moment for “*Ca. M. multicellularis*” in two different magnetic fields. Solid symbols correspond to a magnetic field of 4 Oe and hollow symbols to a magnetic field of 15 Oe. It is also seen a positive correlation in both cases ($r = 0.77$ and significance $p < 0.0001$ for 4 Oe and $r = 0.62$ and significance $p = 0.0002$ for 15 Oe)

Those values are greater than the values obtained for *M. magneticum* strain AMB-1 bacteria. That difference must be due to different flagellar apparatus among both bacteria, and also because *M. magneticum* strain AMB-1 lives in a medium rich in nutrients, different from the environment where the uncultured MTB cocci was maintained. Also, Pierce et al. [11] observed that P_{Fla} had a positive correlation with the magnetic moment. Our data also showed a positive correlation among the magnetic moment and F_{Fla} and P_{Fla} for several values of magnetic field intensity in “*Ca. M. multicellularis*” and the uncultured MTB cocci (Fig. 8).

On the other hand, for “*Ca. M. multicellularis*” the situation observed here was different. Table 4 shows that the flagellar thrust F_{Fla} , the power output of the flagella P_{Fla} and the kinetic

energy K had a dependence on the magnetic field intensity. Those parameters increased with the magnetic field. That can be interpreted as the magnetic field doing a force on the “*Ca. M. multicellularis*” body. For the uncultured MTB cocci that force was not observed because the bacterial body has a single magnetic moment immersed in a uniform magnetic field. On the other hand, “*Ca. M. multicellularis*” had a distribution of magnetic moments, each lying on a spherical helix. The “*Ca. M. multicellularis*” body must experience a magnetic force in the form of

$$\mathbf{F}_{\text{Mag}} = \text{Grad}(m \cdot B \cdot \cos \varphi) = m \cdot B \cdot \text{Grad}(\cos \varphi) \quad (14)$$

where Grad is the gradient operator. According to the model of Acosta-Avalos et al. [23], the angle φ between each magnetic moment located on a tangent plane to the helical curve and the magnetic field changes continuously. However, for symmetry considerations, the total force must be null in the entire body because φ starts increasing from some initial value, get a maximum value and then decreases to return back to the initial value. Silva [19] observed that some cells in “*Ca. M. multicellularis*” may not present magnetosome chains. In some cases, only half of the cells composing “*Ca. M. multicellularis*” presented magnetosome chains. For those cases $\mathbf{F}_{\text{Mag}} \neq \mathbf{0}$ and an increase in the average velocity must be observed when the magnetic field increases as was observed here (Table 1). The presence of this magnetic force explains well the increase in velocity of “*Ca. M. multicellularis*” when the magnetic field increases, as reported in references [6, 7]. The effect of this force has never been reported because until the present moment the parameters associated with the movement’s dynamic were never analyzed as a function of the magnetic field intensity for “*Ca. M. multicellularis*.” As \mathbf{F}_{Mag} increases with the magnetic field, its effects must be ignorable in the presence of the geomagnetic field and our comprehension of magnetotaxis must continue the same for low magnetic fields in the multicellular magnetotactic prokaryote “*Ca. M. multicellularis*.”

4 Conclusion

The present manuscript studied the movement of magnetotactic microorganisms by videomicroscopy with enough resolution to measure their dimensions and to permit the analysis of diverse dynamical parameters as the drag rotational coefficient f_v , the kinetic energy K , the flagellar force F_{Fla} and the flagellar output power P_{Fla} . De Melo et al. [10] analyzed the movement of the same uncultured MTB cocci and “*Ca. M. multicellularis*” for magnetic fields lower than 1 Oe and observed that the magnetotactic response presented by each one is different. Our results also showed that both magnetotactic microorganisms present different behaviors. While the uncultured MTB cocci presented constant values for the kinetic energy, flagellar force and flagellar output power, “*Ca. M. multicellularis*” presented those parameters depending on the magnetic field intensity. For the uncultured MTB cocci, the effective temperature T_{Eff} presented different values for $B < 5$ Oe and $B > 5$ Oe, different than the T_{Eff} for “*Ca. M. multicellularis*” that maintained a constant value. In common, both microorganisms showed higher values of drag rotational coefficient f_v than the expected theoretical value. As far as we know, for the first time that discrepancy was understood as an extra drag produced by the motion in a helical trajectory, producing an “effective radius” for the microorganism. The differences observed among both microorganisms must be related to the multicellular nature of “*Ca. M. multicellularis*” whose magnetic moment distribution is probably able to produce a magnetic force in the presence of a uniform magnetic field.

In conclusion, the present manuscript challenged the idea of the kinetic energy K being constant for multicellular magnetotactic prokaryotes. In that case, K is not constant and

depends on the magnetic field differently from what happens in unicellular MTB where K is constant. Also, the manuscript studied the dynamical parameters of motion of uncultured MTB cocci and “*Ca. M. multicellularis*,” obtaining values for several dynamical parameters that must support future studies and models on the motion of microorganisms under very low Reynolds number.

Acknowledgements Ana Luiza Carvalho thanks Brazilian agency CNPq by PIBIC Grant. Fernanda Abreu acknowledges CNPq, CAPES and FAPERJ funding agencies. We thank the microscopy facilities CENABIO-UFRJ and UniMicro-UFRJ.

Data Availability Statement All data are available under request.

Author contributions DAA collected samples of *Ca. M. multicellularis* and uncultured MTB cocci. FA performed transmission electron microscopy observation in uncultured MTB cocci. Videos of microorganism movement were obtained by ALC and DAA. ALC analyzed all the videos to obtain the trajectory parameters. DAA carried out all the data analyzes and drafted the manuscript. FA critically revised the manuscript. All authors gave final approval for publication.

Funding Not applicable.

Compliance with ethical standards

Conflict of interest The authors declare no conflict of interest.

References

1. R.P. Blakemore, Ann. Rev. Microbiol. **36**, 217–238 (1982)
2. Y. Pan, C. Deng, Q. Liu, N. Petersen, R. Zhu, Chin. Sci. Bull. **49**, 2563–2568 (2004)
3. A.J. Kalmijn, IEEE Trans. Mag. **17**, 1113–1124 (1981)
4. R. Uebe, D. Schuler, Nat. Rev. Microbiol. **14**, 621–637 (2016)
5. C.N. Keim, R.D. De Melo, F.P. Almeida, H.G.P. Lins de Barros, M. Farina, D. Acosta-Avalos, Environ. Microbiol. Rep. **10**, 465–474 (2018)
6. F.P. Almeida, N.B. Viana, U. Lins, M. Farina, C.N. Keim, Antonie van Leeuwenhoek **103**, 845–857 (2013)
7. R.D. De Melo, D. Acosta-Avalos, Antonie Van Leeuwenhoek **110**, 177–186 (2017)
8. M.P. Pichel, T.A.G. Hageman, I.S.M. Khalil, A. Manz, L. Abelmann, J. Magn. Magn. Mater. **460**, 340–353 (2018)
9. D. Acosta-Avalos, E. Rodrigues, Eur. Biophys. J. **48**, 691–700 (2019)
10. R.D. De Melo, P. Leão, F. Abreu, D. Acosta-Avalos, Antonie Van Leeuwenhoek **113**, 197–209 (2020)
11. C.J. Pierce, E. Osborne, E. Mumper, B.H. Lower, S.K. Lower, R. Sooryakumar, Biophys. J. **117**, 1250–1257 (2019)
12. U. Lins, F. Freitas, C.N. Keim, H. Lins de Barros, D.M.S. Esquivel, M. Farina, Braz. J. Microbiol. **34**, 111–116 (2003)
13. D.M.S. Esquivel, H.G.P. Lins de Barros, J. Exp. Biol. **121**, 153–163 (1986)
14. C.N. Keim, J.L. Martins, H. Lins de Barros, U. Lins, M. Farina, in *Magnetoreception and Magnetosomes in Bacteria*, ed. by D. Schuler (Springer-Verlag, Berlin, 2006), pp. 103–132
15. G. Lowe, M. Meister, H.C. Berg, Nature **325**, 637–640 (1987)
16. B. Devouard, M. Posfai, X. Hua, D.A. Bazylinski, R.B. Frankel, P.R. Buseck, Am. Mineral. **83**, 1387–1398 (1998)
17. D. Acosta-Avalos, A.C. Figueiredo, C.P. Conceição, J.J.P. da Silva, K.J.M.S.P. Aguiar, M.L. Medeiros, M. Nascimento, R.D. De Melo, S.M.M. Sousa, H. Lins de Barros, O.C. Alves, F. Abreu, Eur. Biophys. J. **48**, 513–521 (2019)
18. F. Abreu, J.L. Martins, T.S. Silveira, C.N. Keim, H.G.P. Lins de Barros, F.J. Gueiros Filho, U. Lins, Int. J. Syst. Evol. Microbiol. **57**, 1318–1322 (2007)

19. K.T. Silva, Master Thesis, Instituto de Microbiologia Professor Paulo de Góes. Universidade Federal do Rio de Janeiro. Rio de Janeiro. Brazil. (2008), p. 27
20. M.R. Spencer, J.M.D. Coey, A.H. Morrish, *Can. J. Phys.* **50**, 2313–2326 (1972)
21. B.R. Heywood, D.A. Bazylinski, A. Garratt-Reed, S. Mann, R.B. Frankel, *Naturwissenschaften* **77**, 536–538 (1990)
22. M. Winklhofer, L.G. Abraçado, A.F. Davila, C.N. Keim, H.G.P. Lins de Barros, *Biophys. J.* **92**, 661–670 (2007)
23. D. Acosta-Avalos, L.M.S. Azevedo, T.S. Andrade, H. Lins de Barros, *Eur. Biophys. J.* **41**, 405–413 (2012)
24. C.N. Keim, F. Abreu, U. Lins, H. Lins de Barros, M. Farina, *J. Struct. Biol.* **145**, 254–262 (2004)
25. R.D. De Melo, D. Acosta-Avalos, *Eur. Biophys. J.* **46**, 533–539 (2017)
26. F.S. Nogueira, H.G.P. Lins de Barros, *Eur. Biophys. J.* **24**, 13–21 (1995)
27. K.T. Silva, F. Abreu, F.P. Almeida, C.N. Keim, M. Farina, U. Lins, *Microsc. Res. Technol.* **70**, 10–17 (2007)
28. K. Bente, S. Mohammadinejad, M.A. Charsooghi, F. Bachmann, A. Codutti, C.T. Lefevre, S. Klumpp, D. Faivre, *eLife* **9**, e47551 (2020)
29. H.C. Crenshaw, *Am. Zool.* **36**, 608–618 (1996)
30. R. Nadkarni, S. Barkley, C. Fradin, *PLoS ONE* **8**, e82064 (2013)
31. X. Mao, R. Egli, N. Petersen, M. Hanzlik, X. Zhao, *Geochem. Geophys. Geosyst.* **15**, 255–283 (2014)
32. C. Rosenblatt, F. Torres de Araujo, R.B. Frankel, *Biophys. J.* **40**, 83–85 (1982)
33. M. Perantoni, D.M.S. Esquivel, E. Wajnberg, D. Acosta-Avalos, G. Cernicchiaro, H. Lins de Barros, *Naturwissenschaften* **96**, 685–690 (2009)
34. X.J. Zhu, X. Ge, N. Li, L.F. Wu, C.X. Luo, Q. Ouyang, Y. Tu, G. Chen, *Integr. Biol.* **6**, 706–713 (2014)
35. K.C. Marshall, R. Stout, R. Mitchell, *J. Gen. Microbiol.* **68**, 337–348 (1971)
36. H. Xin, Q. Liu, B. Li, *Sci. Rep.* **4**, 6576 (2014)
37. C. Yang, C. Chen, Q. Ma, L.F. Wu, T. Song, *J. Bionic Eng.* **9**, 200–210 (2012)